collection experiment; and to A. Habenschuss, Oak Ridge Associated Universities, for his help in performing the latter.

References

BORLERA, M. L. & PRADELLI, G. (1971). *Metall. Ital.* **63**, 107–111.
BROWN, G. M. & CHIDAMBARAM, R. (1969). *Acta Cryst.* B25, 676–687.
BUNGARDT, K., KUNZE, E. & HORN, E. (1958). *Arch. Eisenhuettenwes.* **29**, 393–394.
BURDESE, A., PRADELLI, G. & GIANOGLIO, C. (1977). *Metall. Ital.* **69**, 487–492.
COPPENS, P. & HAMILTON, W. C. (1970). *Acta Cryst.* A26, 71–83.
CORFIELD, P. W. R., DOEDENS, R. J. & IBERS, J. A. (1967). *Inorg. Chem.* **6**, 197–200.
CROMER, D. T. (1983). *J. Appl. Cryst.* **16**, 437.
CROMER, D. T. & LIBERMAN, D. (1970). *Relativistic Calculation of Anomalous-Scattering Factors for X-rays.* Report LA-4403. Los Alamos Scientific Laboratory, New Mexico.
GLOWACKI, Z., BAER, J. & LEDA, H. (1968). *J. Iron Steel Inst.* **206**, 393–394.
HAMILTON, W. C. (1965). *Acta Cryst.* **18**, 502–510.
International Tables for X-ray Crystallography (1974). Vol. IV. Birmingham: Kynoch Press. (Present distributor D. Reidel, Dordrecht.)

KUO, K. (1953). *Jernkontorets Ann.* **137**, 149–156.
LAI, J. K. L. & MESHKAT, M. (1978). *Met. Sci.* **12**, 415–420.
MEINHARDT, D. & KRISEMENT, O. (1962). *Arch. Eisenhuettenwes.* **33**, 493–499.
PAULING, L. (1960). *The Nature of the Chemical Bond*, 3rd ed., pp. 393–448. Ithaca, NY: Cornell Univ. Press.
SAMSON, S. (1964). *The Structure of Metals and Intermetallic Compounds*, Sept. 1, 1953–Aug. 31, 1964. Final Report, ONR Contract Nonr-220-33. California Institute of Technology, Pasadena.
SHAW, S. W. & QUARRELL, A. G. (1957). *J. Iron Steel Inst.* **185**, 10–22.
SHOEMAKER, D. P. (1966). *World List of Crystallographic Computer Programs*, 2nd ed. Utrecht: Oosthoek.
STADELMEIER, H. H. (1969). *Metal-Rich Metal-Metalloid Phases*, pp. 141–180, in *Developments in the Structural Chemistry of Alloy Phases*, edited by B. C. GIESSEN. New York: Plenum Press.
TEMPLETON, L. K., TEMPLETON, D. H., PHIZACKERLEY, R. P. & HODGSON, K. O. (1982). *Acta Cryst.* A38, 74–78.
WESTGREN, A. (1933). *Jernkontorets Ann.* **117**, 501–512.
WESTGREN, A., PHRAGMÉN, G. & NEGRESCO, TR. (1928). *J. Iron Steel Inst.* **117**, 383–406.
YAKEL, H. L. (1982). *Scripta Metall.* **16**, 453–454.
YAKEL, H. L. (1983a). *Acta Cryst.* B39, 20–28.
YAKEL, H. L. (1983b). *Acta Cryst.* B39, 28–33.

Studies of K₃Nb₇O₁₉ by High-Resolution Electron Microscopy and X-ray Powder Diffraction

BY MARGARETA SUNDBERG AND MONICA LUNDBERG

Department of Inorganic Chemistry, Arrhenius Laboratory, University of Stockholm, S-106 91 Stockholm, Sweden

Abstract

An idealized structure model of the $K_3Nb_7O_{19}$ compound has been deduced from high-resolution electron micrographs. For simplicity the structure was derived in a pseudo-monoclinic system with triclinic symmetry (space group $P\bar{1}$) and unit-cell dimensions $a = 13.777$ (2), $b = 6.431$ (1), $c = 18.897$ (6) Å, $\alpha \simeq 90$, $\beta = 98.06$ (2) and $\gamma \simeq 90°$, $V = 1657.7$ Å^3, $Z = 4$. It has been verified both by simulated image calculations in two projections and by X-ray powder diffraction studies. The structure consists of a three-dimensional framework which is built up of pairs of NbO_6 octahedra having one edge in common in such a way that the structure can be described by means of $\{011\}$ crystallographic shear in the ReO_3 type structure. The pairs are linked by edge and corner sharing as in the $\{120\}$ crystallographic-shear (CS) structure M_7O_{20}. Two kinds of tunnels are formed, in which the K atoms are located. The structure thus independently derived agrees with that recently published by Fallon, Gatehouse & Guddat [*J. Solid State Chem.* (1986), **61**, 181–189], which was determined from single-crystal X-ray data, although their unit cell is

triclinic. We have refined the cell parameters given in that article: $a = 14.1282$ (9), $b = 9.9369$ (9), $c = 6.4553$ (6) Å, $\alpha = 106.44$ (1), $\beta = 95.856$ (6) and $\gamma = 97.30$ (1)°, $V = 853.05$ Å^3, $Z = 2$, $M_r = 1071.64$, and $D_x = 4.17$ g cm^{-3}. However, in this paper the structure is described in a different manner and discussed in relation to neighbouring compounds of this system. The JCPDS Diffraction File No. for $K_3Nb_7O_{19}$ is 38-1499.

Introduction

High-resolution electron microscopy (HREM) studies of some phases occurring in the $KNbO_3$–Nb_2O_5 system have recently been published (Lundberg & Sundberg, 1986). That article is focused on three different types of tetragonal tungsten bronze (TTB) structure and a block structure, $KNb_{13}O_{33}$. In addition to these compounds, there exist two kinds of layer structures, namely $K_4Nb_6O_{17}$ (Gasperin & Le Bihan, 1982) and L-KNb_3O_8 (Gasperin, 1982), both determined by single-crystal X-ray diffraction. A survey of the $KNbO_3$–Nb_2O_5 system published by Roth, Parker, Brower & Minor (1974) included

several of the compounds mentioned above as well as a triclinic phase which was assigned the composition $K_8Nb_{18}O_{49}$.

In the course of our phase-analysis studies, a supposedly new compound, triclinic with the stoichiometry $K_3Nb_7O_{19}$, was identified both by Guinier X-ray powder diffraction and by electron optical methods. A structure model could be derived from HREM images in two axial projections.

In the final stage of the investigation, an X-ray single-crystal structure determination of $K_3Nb_7O_{19}$ appeared in the literature (Fallon, Gatehouse & Guddat, 1986). The results reported in that article confirmed our structure model. However, it seems worthwhile to publish these results, as we have used a combination of HREM and X-ray powder techniques. Some attention will be paid to the problems we met by combining the HREM and X-ray powder results. This study will also provide an example of the accuracy that can be achieved in deriving atomic positions of a three-dimensional structure model from HREM images in two projections. We also show that the structure can be derived from an ReO_3-type basic framework and described in terms of crystallographic shear in two dimensions. Hypothetical homologues can also be proposed. As distinguished from the discussion given by Fallon *et al.* (1986), our discussion will emphasize relationships to structures of neighbouring compounds in the K–Nb–O system.

Experimental

The sample was prepared from a mixture of Nb_2O_5 and $KNbO_3$ in the mole ratio 2:3. Nb_2O_5 (Merck, optipure) was purified from oxide fluorides in air at 1375 K, and $KNbO_3$ was obtained by heating equimolar amounts of K_2CO_3 (BDH, Laboratory reagents) and Nb_2O_5 at 1175 K for two days. The mixture was heated in a sealed platinum tube at 975 K for one day and at 1325 K for five days.

The compound was microcrystalline and colourless. X-ray powder photographs were taken in a focusing camera of Guinier–Hägg type with monochromatized Cu $K\alpha_1$ radiation. The films were analysed with a film-scanner measuring system (Johansson, Palm & Werner, 1980). The unit-cell parameters were refined with the program *PIRUM* (Werner, 1969) using silicon as an internal standard [$a/\lambda = 3.525\,176$ (Hubbard, Swanson & Mauer 1975)].

The sample was studied by electron-optical and HREM techniques (Spence, 1981). The preparation of the electron-microscopy samples has previously been described (Lundberg & Sundberg, 1986). The specimens were examined in a JEOL 200CX electron microscope equipped with an ultra-high-resolution top-entry goniometer stage with tilt angles of $\pm10°$. The microscope was operated at 200 kV. The spherical

aberration constant was 1·2 mm, and the semi-angle of the beam convergence was 5 mrad. All images were taken using an objective aperture with a radius corresponding to $0.41\,\text{Å}^{-1}$ in reciprocal space.

Electron diffraction (ED) patterns were recorded of thin crystal flakes aligned in several orientations. From these ED patterns attempts were made to find a unit cell which conformed to the Guinier powder pattern of the $K_3Nb_7O_{19}$ phase. HREM images were recorded at different defocus values of those flakes which from the ED patterns seemed to have the most favourable orientations with respect to the substructure. According to HREM theory, the contrast in micrographs of thin well aligned crystal fragments at optimal defocus (Scherzer focus) can be interpreted in terms of the projected potential and thus the atomic configuration.

Simulated images were calculated by using an updated version of the *SHRLI* suite of programs (O'Keefe, Buseck & Iijima, 1978). Calculations were made for different crystal thicknesses and different defocus values. An image processing system (Kontron IBAS II/IPS) was used to combine simulated and observed images.

Results and discussion

The electron-microscopy study showed that information on the crystal structure of the phase could be obtained both from the ED pattern and the corresponding HREM image when a thin crystal flake was aligned as in Fig. 1(*a*). From this ED pattern, which is the [010] zone, approximate lattice constants were calculated to be $a = 13.9$, $c = 9.4\,\text{Å}$ and $\beta = 98.5°$. As can be seen from Fig. 1(*a*), singlets or doublets of strong substructure reflection spots are located close to the intersection points of a rectangular sublattice, whose cell dimensions suggest that the structure is related to the ReO_3 type. From the position of the first Laue zone observed in an overexposed ED pattern along [010], the length of the projection axis was calculated to be roughly $6.3\,\text{Å}$. This value was confirmed from the ED pattern in Fig. 1(*b*). From this $(0kl)$ projection, the lattice can be chosen in two alternative ways: either as having the dimensions $b \simeq 6.4$, $c \simeq 18.9\,\text{Å}$ and $\alpha \simeq 90°$ or $b \simeq 6.3$, $c \simeq 9.9\,\text{Å}$ and $\alpha \simeq 107°$. These dimensions, together with the ones obtained from the $(h0l)$ projection, could be interpreted as a pseudo-monoclinic unit cell, *i.e.* with α and γ very close to 90°, or as a triclinic cell with $\alpha \simeq 107$, $\beta \simeq 98.5$ and $\gamma \neq 90°$.

Fig. 1(*c*) shows the HREM image of a thin crystal fragment aligned as in Fig. 1(*a*). The contrast in the micrograph can be described as rows consisting of seven black spots and mutually connected so that groups of four black spots are formed. The groups are separated by white dots and form straight lines in the image. These image features together with the
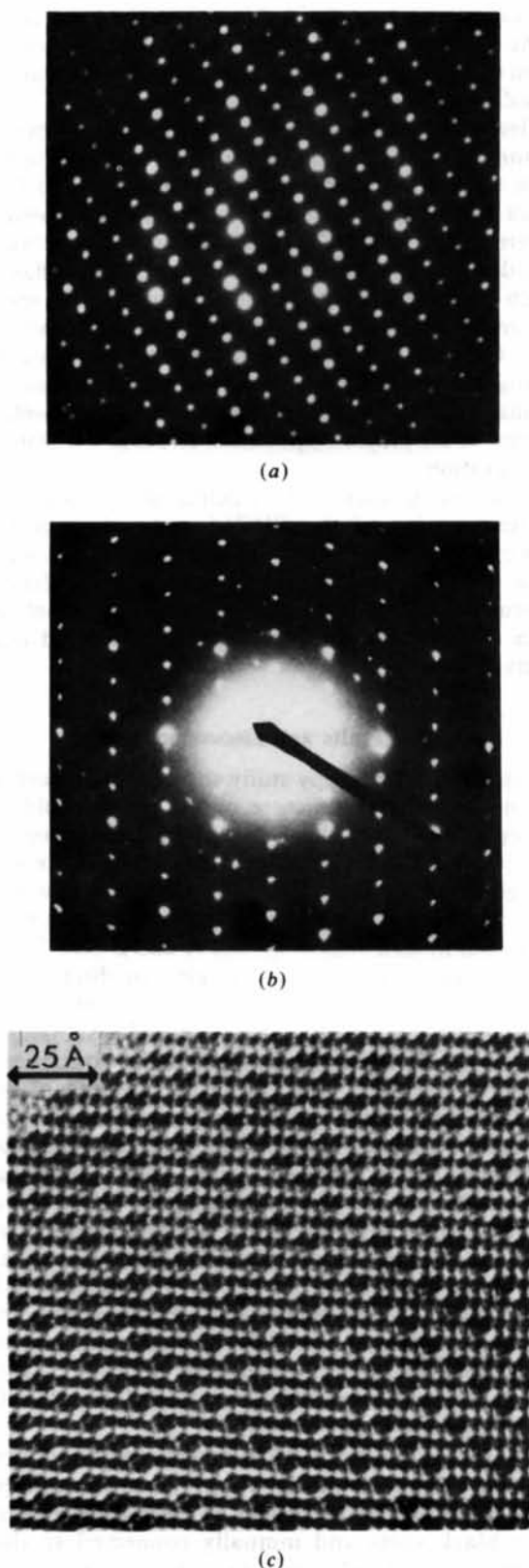
(a)

(b)

(c)

Fig. 1. The structure of $K_3Nb_7O_{19}$. (a) ED pattern along [010]. (b) ED pattern along [100]. (c) HREM image along [010].

ED pattern in Fig. 1(a) suggested that the structure might in some way be related to the crystallographic-shear (CS) structures. The distance across the seven black spots indicated that the spots might be interpreted as seven corner-sharing NbO_6 octahedra. The groups of four black spots might indicate edge sharing of NbO_6 octahedra as in the {120} CS structures.

However, it was apparent from the distance across two rows of black spots, as well as from their size and shape, that a spot could not simply be interpreted as an NbO_6 octahedron. These facts, and also the length of the projection axis (6·4 Å), showed that the structure was not built up of a simple ReO_3-type framework. The black spot could, instead, be interpreted as a pair of edge-sharing NbO_6 octahedra projected along a common diagonal (Nb_2O_{10} unit). In this projection, the two Nb atoms are too close to be resolved in the HREM image, but spots of the observed shape and size should result in such a contrast. This type of Nb_2O_{10} unit can be found in related structures (see below). The contrast in the micrograph can thus be interpreted as segments of seven pairs of edge-sharing octahedra, mutually linked by corner sharing as seen in Fig. 1(d). These segments are, as assumed above, linked to form groups of eight edge-sharing NbO_6 octahedra. The stoichiometry of the Nb–O framework is $Nb_7O_{19}^{3-}$, which is in agreement
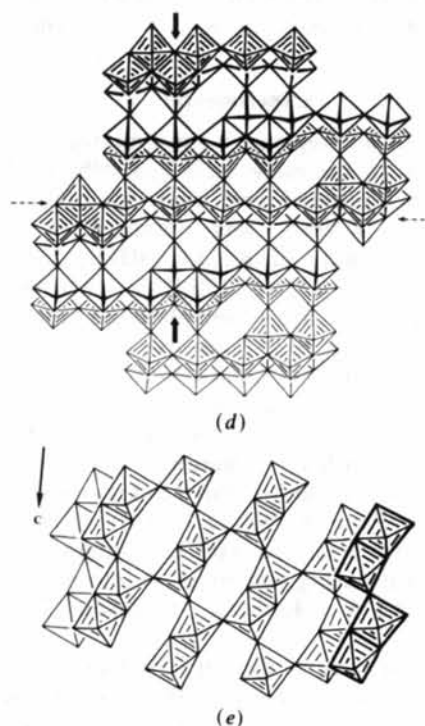

(d)

(e)

Fig. 1 (cont.) (d) Deduced idealized structure model in the (h0l) projection of the pseudo-monoclinic cell corresponding to the (hk0) projection of the triclinic cell. Dashed arrows point to a row of seven Nb_2O_{10} units. (e) A slice of the three-dimensional octahedral framework exposing the connection of NbO_6 octahedra along the c axis, as indicated by solid arrows in (d).

with the synthesis. Three K atoms have to be inserted to obtain electroneutrality.

Starting from this model, approximate atomic parameters were calculated. First, all Nb-atom positions were located in the projection of a monoclinic cell. At an early stage it became obvious that the symmetry must be triclinic in order to generate the atoms correctly and maintain reasonable Nb–Nb distances. The space group $P\bar{1}$ was chosen, although a pseudo-monoclinic unit cell was used.

In order to introduce acceptable O-atom positions in the unit cell, interatomic distances were subsequently calculated. The O atoms in the suggested octahedral network are arranged in a nearly cubic close-packed array, in which some vacancies appear. From this point of view it is reasonable to believe that the K atoms are located at the vacant sites. If this is the case there must be some type of disordered distribution, since there are more vacancies than K atoms in the unit cell. No contrast that could be assigned to K atoms could be observed in the recorded HREM images along [010], so these atoms were assumed to be randomly distributed over the available vacancies. The resulting unit-cell parameters and the atomic coordinates have been deposited.*

Simulated images of the deduced structure model have been calculated and compared with the recorded ones. As can be seen from Fig. 2(a), there is good agreement between observed and calculated images along [010]. The accuracy of the model was also checked by comparison of images in the (0kl) projection. A through-focus set of images is shown in Fig. 2(c). The HREM image is shown in Fig. 2(b). It turned out that the micrograph was probably taken at overfocus (600 Å) instead of at the Scherzer focus and thus had reversed contrast (cf. the experimental image and that calculated at −600 Å). As can be seen from Fig. 2(b), good agreement was obtained between the observed and calculated image with a slight adjustment of the contrast levels. When good

---

* Atomic coordinates and the indexed powder pattern have been deposited with the British Library Document Supply Centre as Supplementary Publication No. SUP 43600 (8 pp.). Copies may be obtained through The Executive Secretary, International Union of Crystallography, 5 Abbey Square, Chester CH1 2HU, England.
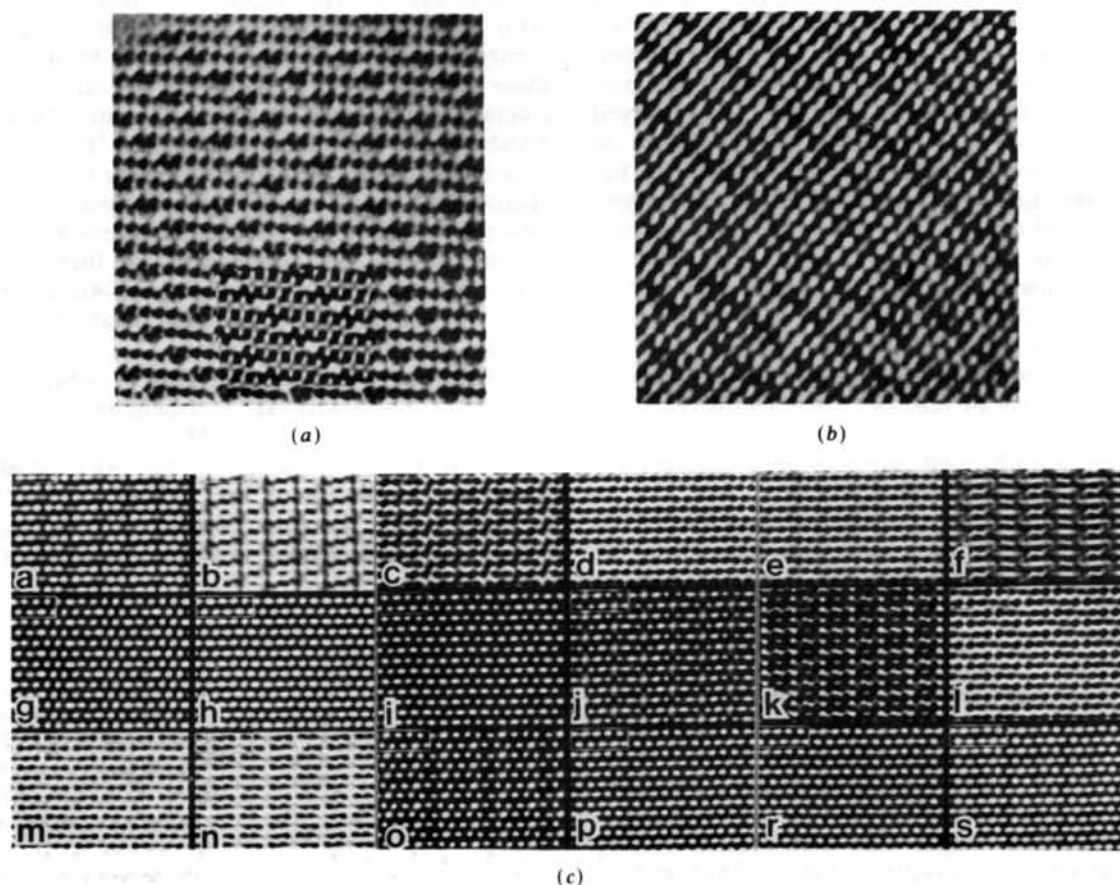

(a)   (b)

(c)

Fig. 2. HREM image of $K_3Nb_7O_{19}$ with calculated images inserted: (a) along [010], thickness = 25·8 Å, defocus −650 Å; (b) along [100], thickness 42 Å, defocus 600 Å. (c) A through-focus set of simulated images along [100], crystal thickness 42 Å, defocus in steps of −100 Å from a 600 Å to s −1100 Å.

agreement between observed and calculated images is obtained in two axial projections, the structure model derived from HREM images can be regarded as essentially correct.

The $K_3Nb_7O_{19}$ phase seems to be strictly stoichiometric, as all recorded ED patterns of thin crystal fragments so far showed sharp reflection spots. No streaking was observed. In accordance with this the micrographs revealed well ordered crystals in which no local defects could be seen.

A Guinier X-ray powder pattern of the compound was procured in order to investigate if the suggested structure model, described with a pseudo-monoclinic unit cell, was also consistent with X-ray diffraction data. All observed reflection lines (144) could be indexed and refined with the monoclinic cell. The cell dimensions obtained were $a = 13.777$ (2), $b = 6.431$ (1), $c = 18.897$ (6) Å and $\beta = 98.06$ (2)°. However, the low figures of merit, $M(20) = 3$ and $F(144) = 6$ (0.019, 1444) (de Wolff, 1968; Smith & Snyder, 1979) indicated that the chosen unit cell was probably not quite correct. There were also inconsistencies between indices of strong reflections in the ED and X-ray patterns. Therefore, a theoretical X-ray powder pattern was calculated, based on the atomic coordinates derived from the HREM image (Fig. 1c). The result displays the same type of powder pattern, with small displacements of the lines. Since our purpose was to find the true unit cell, the observed powder pattern was reindexed as triclinic based on lattice dimensions from the (h0l) projection (Fig. 1a) and the second interpretation of lattice parameters (see above) in the (0kl) projection (Fig. 1b). At this stage an X-ray single-crystal structure determination of $K_3Nb_7O_{19}$ was published by Fallon et al. (1986). The unit-cell dimensions given in that article were used to index the X-ray powder pattern, and the least-squares refinement resulted in the following parameters: $a = 14.1282$ (9), $b = 9.9369$ (9), $c = 6.4553$ (6) Å, $\alpha = 106.44$ (1), $\beta = 95.856$ (6), $\gamma = 97.30$ (1)°. The obtained figures of merit are $M(20) = 12$ and $F(144) = 14$ (0.009, 1305).

To check the accuracy of the structure determination from HREM images, our coordinates of the Nb atoms were transformed from the pseudo-monoclinic to the triclinic cell and compared with those found from the X-ray single-crystal study (Fallon et al., 1986) (Table 1). As can be seen from Table 1, the largest difference between positions found by the two methods was about 0.3 Å. Note that no refinement of the parameters obtained from the HREM study has been made. The relationship between the pseudo-monoclinic and triclinic unit cells is shown in Fig. 3.

The simulated images were then recalculated by using the refined unit-cell parameters of the triclinic cell and the atomic positions reported in the single-crystal X-ray study, as these are of much higher accuracy than those obtained from our micrographs.

Table 1. Nb-*atom coordinates transformed from the pseudo-monoclinic cell to the triclinic unit cell*

As a comparison the Nb-atom coordinates, obtained from X-ray single-crystal data (Fallon et al., 1986), are given within parentheses.

	x	y	z
Nb 1	0.514	0.612	0.420
	(0.5065)	(0.6222)	(0.3659)
Nb 2	0.365	0.234	0.140
	(0.3472)	(0.2176)	(0.1564)
Nb 3	0.265	0.276	0.579
	(0.2583)	(0.2929)	(0.6186)
Nb 4	0.210	0.840	0.997
	(0.1871)	(0.8445)	(0.9908)
Nb 5	0.891	0.108	0.534
	(0.8891)	(0.0928)	(0.5665)
Nb 6	0.428	0.670	0.876
	(0.4193)	(0.6845)	(0.8267)
Nb 7	0.043	0.478	0.720
	(0.0358)	(0.4700)	(0.7762)

Fig. 4 shows the HREM images with the recalculated images inserted. As can be seen from Figs. 2 and 4, there are only minor differences between the two sets of calculated images.

The description of the structure of $K_3Nb_7O_{19}$ can be made either as that given by Fallon et al. (1986) or in terms of crystallographic shear (CS) in an octahedral framework of ReO_3 type. Rows of seven corner-sharing octahedra are linked through {120} shear to form infinite chains. Two such chains are connected by corner sharing to create ribbons of which the entire structure can be built (Fig. 5a). The ribbons are joined through {011} shear in a stepwise manner (Fig. 1d). The sheets thus formed, which are infinite in two directions, are interconnected by corner sharing in the third dimension, so that a three-dimensional octahedral network is obtained. Owing to the shear along {011}, all NbO_6 octahedra appear in pairs (Fig. 1e).

The similarity between the $K_3Nb_7O_{19}$ structure and the {120} CS structure M_7O_{20} [member $n = 7$ of the homologous series M_nO_{3n-1} (Magnéli, 1953)] can be seen from Figs. 1(d) and 5(b). In Fig. 5(b), the M_7O_{20} structure is built up of the ribbons in Fig. 5(a) mutually linked by corner sharing. The layers, one octahedron thick, formed in this fashion are stacked
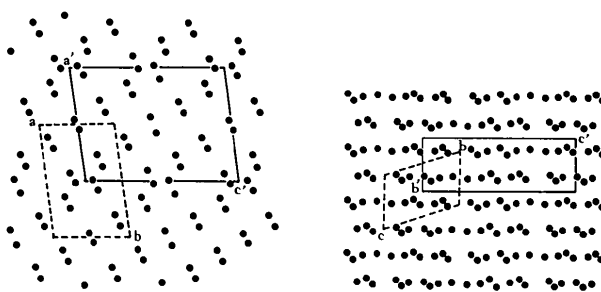

Fig. 3. The projections of Nb atoms in two directions show the relation between the pseudo-monoclinic (solid) and the triclinic (dashed) unit cells.

one on top of the other and joined by corners. Substitution of every octahedron in the M_7O_{20} structure by an M_2O_{10} unit will not change the O/M ratio, but formation of the group of four edge-linked M_2O_{10} units eliminates one O atom per M_7O_{20} unit. Thus, the stoichiometry of the structure formed will be M_7O_{19}. With $M = Nb^V$, electroneutrality requires addition of three positive charges; with K atoms inserted, this will give the formula $K_3Nb_7O_{19}$.

From Fig. $1(d)$, it is apparent that other phases with related structures might be formed. For example, structures built up of rows of six or eight corner-sharing MO_6 octahedra, instead of seven, can be proposed. By analogy with the previously known CS structures, a new type of homologous series, $A_xM_nO_{3n-2}$ (A = alkali), based on both {120} and {011} crystallographic shear can be formulated, where the $K_3Nb_7O_{19}$ phase can be regarded as the first observed member ($n = 7$). The members $n = 6$ and $n = 8$ will have the formulas KNb_3O_8 and $K_2Nb_4O_{11}$, respectively. So far these two CS structures have not been observed in the K–Nb–O system. KNb_3O_8 is known to form both a layer-type structure at low

temperature (Gasperin, 1982) and a tetragonal tungsten-bronze-related structure at high temperature (Lundberg & Sundberg, 1986). The reason why the KNb_3O_8 phase prefers to adopt these two structure types instead of the shear structure might be answered by lattice-energy-minimization calculations. Such studies are in progress.

The type of pairs of edge-linked octahedra described above can be recognized in many structures such as $CaTa_2O_6$ (Jahnberg, 1963) and $K_4Nb_6O_{17}$ (Gasperin & Le Bihan, 1982). However, the pairs of octahedra in the former compound are coupled
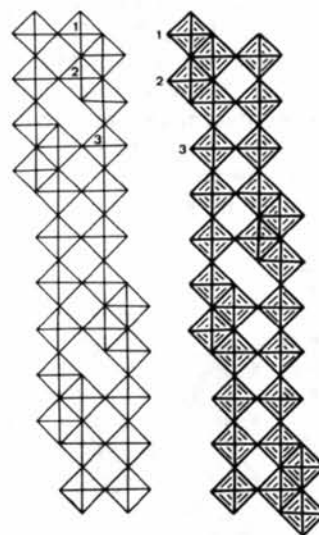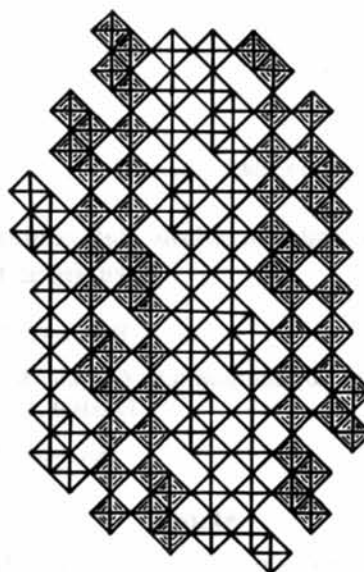

(a)
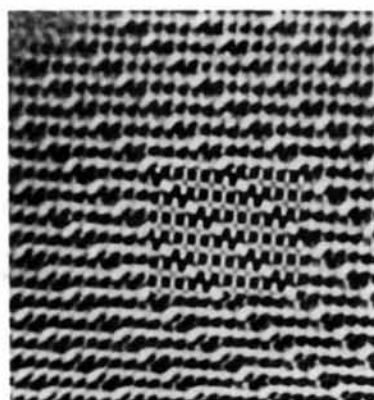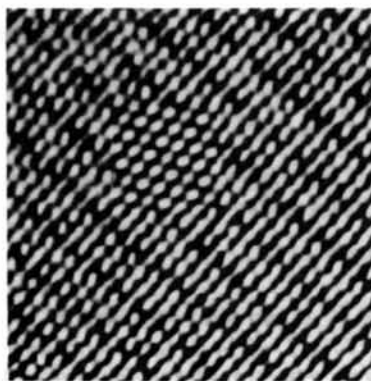
Fig. 4. The HREM images with the recalculated image (triclinic cell) inserted: (a) along [010], thickness 25·8 Å, defocus −650 Å; (b) along [100], thickness 42 Å, defocus 600 Å.

(a)

(b)

Fig. 5. (a) Idealized one-dimensional infinite ribbons of corner- and edge-sharing NbO_6 octahedra. The numbers refer to O atoms joining the ribbons to a two-dimensional sheet through {011} shear. (b) The {120} CS structure M_7O_{20}.

exclusively by corner sharing and the pairs are tilted relative to each other.

Large structural similarities between the compounds $K_4Nb_6O_{17}$ and $K_3Nb_7O_{19}$ can be noticed, especially the stacking sequence of the pairs of octahedra along the short axis (6·4 Å). The structure of $K_4Nb_6O_{17}$ projected along this short axis shows that the $Nb_6O_{17}^{4-}$ layers are built of three edge-sharing Nb_2O_{10} units (Fig. 6), while projection of $K_3Nb_7O_{19}$ shows four edge-sharing units together with units which are exclusively corner sharing.

A triclinic phase with a composition very close to that of $K_3Nb_7O_{19}$ has been published by Roth *et al.* (1974). The formula is given as $K_8Nb_{18}O_{49}$ but can also be written as $K_{3·10}Nb_{6·98}O_{19}$. The unit-cell dimensions reported for $K_8Nb_{18}O_{49}$ were used to index our Guinier X-ray powder diffraction film. Refinement of the parameters resulted in a unit cell with $a = 13·356 (9)$, $b = 13·93 (1)$, $c = 15·03 (1)$ Å, $\alpha = 82·24 (5)$, $\beta = 69·54 (6)$ and $\gamma = 89·18 (5)°$; very similar to that given by Roth *et al.*, but the figures of
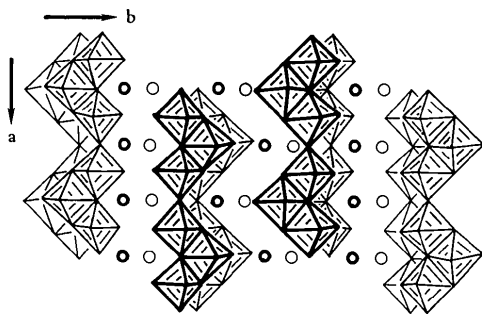

Fig. 6. Projection of the structure of $K_4Nb_6O_{17}$ along the *c* axis (6·46 Å). The $Nb_6O_{17}^{4-}$ layers contain three pairs of edge-sharing octahedra mutually joined by corner sharing. The layers are interleaved by K^+ ions.

merit were poor, $M(20) = 2$, $F(144) = 5 (0·013, 2461)$. Therefore, it is reasonable to believe that the specimen reported as $K_8Nb_{18}O_{49}$ is essentially the $K_3Nb_7O_{19}$ phase.

This demonstrates the importance of calculating the figures of merit when deriving unit cells with low symmetry from complex powder patterns such as this.

References

FALLON, G. D., GATEHOUSE, B. M. & GUDDAT, L. (1986). *J. Solid State Chem.* **61**, 181–189.
GASPERIN, M. (1982). *Acta Cryst.* **B38**, 2024–2026.
GASPERIN, M. & LE BIHAN, M. T. (1982). *J. Solid State Chem.* **43**, 346–353.
HUBBARD, C. R., SWANSON, H. E. & MAUER, F. A. (1975). *J. Appl. Cryst.* **8**, 45–48.
JAHNBERG, L. (1963). *Acta Chem. Scand.* **17**, 2548–2559.
JOHANSSON, K.-E., PALM, T. & WERNER, P.-E. (1980). *J. Phys. E*, **13**, 1289–1291.
LUNDBERG, M. & SUNDBERG, M. (1986). *J. Solid State Chem.* **63**, 216–230.
MAGNÉLI, A. (1953). *Acta Cryst.* **6**, 495–500.
O'KEEFE, M., BUSECK, P. R. & IIJIMA, S. (1978), *Nature (London)*, **274**, 322–324.
ROTH, R. S., PARKER, H. S., BROWER, W. S. & MINOR, D. (1974). *Alkali Oxide-Tantalum Oxide and Alkali Oxide-Niobium Oxide Ionic Conductors.* NASA Tech. Rep. CR 134599.
SMITH, G. S. & SNYDER, R. L. (1979). *J. Appl. Cryst.* **12**, 60–65.
SPENCE, J. C. H. (1981). *Experimental High-Resolution Electron Microscopy.* Oxford: Clarendon Press.
WERNER, P.-E. (1969). *Ark. Kemi*, **31**, 513–516.
WOLFF, P. M. DE (1968). *J. Appl. Cryst.* **1**, 108–113.

Strontium and Europium Polynuclear Units in Intermetallic Compounds with Magnesium. Structural Refinements and Relationships

BY JÖRG ERASSME AND HEIKO LUEKEN*

Institut für Anorganische Chemie der Technischen Hochschule Aachen, Professor-Pirlet-Strasse 1, D-5100 Aachen, Federal Republic of Germany

Abstract

The crystal structures of $(Sr_{0·67}Eu_{0·33})_3Mg_{13}$ [$M_r = 642·61$, hexagonal, $P6_3/mmc$, $a = 10·465 (3)$, $c = 28·166 (5)$ Å, $V = 2671 (2)$ Å^3, $Z = 6$, $D_x = 2·40$ Mg m^{-3}, $\lambda(Mo K\alpha) = 0·71069$ Å, $\mu = 9·5$ mm^{-1}, $F(000) = 1770$, $T = 294$ K, final R value 0·026 for 567 independent reflections] and $EuMg_{5·2}$ [$M_r = 278·38$, hexagonal, $P6_3/mmc$, $a = 10·395 (3)$, $c = 10·746 (3)$ Å, $V = 1005·6 (9)$ Å^3, $Z = 6$, $D_x = 2·76$ Mg m^{-3}, $\lambda(Mo K\alpha) = 0·71069$ Å, $\mu = 9·6$ mm^{-1}, $F(000) = 752·4$, $T = 294$ K, final R value 0·026 for

* Author to whom correspondence should be addressed.